Strong correlation effects in the *A*-site ordered perovskite $CaCu_3Ti_4O_{12}$ revealed by angle-resolved photoemission spectroscopy

H. J. Im,[1,*] M. Tsunekawa,[2] T. Sakurada,[1] M. Iwataki,[1] K. Kawata,[1] T. Watanabe,[1] K. Takegahara,[1] H. Miyazaki,[3] M. Matsunami,[4,5] T. Hajiri,[4,6] and S. Kimura[4,5,7]

[1]*Department of Advanced Physics, Hirosaki University, Hirosaki 036-8224, Japan*
[2]*Faculty of Education, Shiga University, Otsu 520-0862, Japan*
[3]*Center for Fostering Young and Innovative Researchers, Nagoya Institute of Technology, Nagoya 466-8555, Japan*
[4]*UVSOR Facility, Institute for Molecular Science, Okazaki 444-8585, Japan*
[5]*School of Physical Sciences, The Graduate University for Advanced Studies, Okazaki 444-8585, Japan*
[6]*Graduate School of Engineering, Nagoya University, Nagoya 464-8603, Japan*
[7]*Graduate School of Frontier Biosciences, Osaka University, Suita 565-0871, Japan*

(Received 21 March 2013; published 22 November 2013)

We report angle-resolved photoemission spectroscopy results of *A*-site ordered perovskite $CaCu_3Ti_4O_{12}$. We have observed the clear band dispersions, which are shifted to the higher energy by 1.7 eV and show the band narrowing around 2 eV in comparison with the local density approximation calculations. In addition, the high-energy multiplet structures of Cu $3d^8$ final states have been found around 8–13 eV. These results reveal that $CaCu_3Ti_4O_{12}$ is a Mott-type insulator caused by the strong correlation effects of the Cu $3d$ electrons well hybridized with O $2p$ states. Unexpectedly, there exists a very small spectral weight at the Fermi level in the insulator phase, indicating the existence of isolated metallic states.

DOI: 10.1103/PhysRevB.88.205133 PACS number(s): 71.30.+h, 79.60.−i

I. INTRODUCTION

A-site ordered perovskite $CaCu_3Ti_4O_{12}$ (CCTO) has generated considerable interest due to the extremely high dielectric constant (ϵ) as high as 10^4–10^5 over a wide range of temperature from 100 to 600 K, which holds promise for a high performance capacitor.[1] Prior to applications, there have been many studies to identify the intrinsic mechanism of the high ϵ. Although the consistent conclusion of the origin has not been established yet, it has been widely accepted that the high ϵ would come from defects and/or disorder structures, e.g., a relaxorlike dipole fluctuation in nanosize domain,[2] an internal barrier layer capacitance,[3] and the nanoscale disorder of Ca and Cu sites.[4] Generally, the origin of the high ϵ of CCTO has been considered to be different from that of conventional ferroelectric materials, because of the absence of structural transition accompanying the abrupt change of ϵ around 100 K.[5,6] Therefore, in order to understand these intriguing physical properties, the electronic structures should be clarified experimentally. In particular, relations between the electronic structure and the strong correlation effects are central issues.[7–9] For example, the high ϵ and an insulator phase of CCTO cannot be explained by theoretical calculations within the local density approximation (LDA), which are not considered to properly treat the strong correlation between electrons. The strong correlation effects can also be expected from the crystal structure of CCTO, which contains the CuO_4 plane units similar to the CuO_2 plane of the high-T_c cuprates as shown in Fig. 1(b).[10] Recently, it has been reported that a family compound, $CaCu_3Ru_4O_{12}$, shows the heavy fermion behavior and the non-Fermi liquid, supporting the importance of the strong correlation effects.[11] Hence, it has been believed that CCTO would be a Mott-type insulator, even though the experimental band dispersions have never been observed. Here, we report the clear observation of band dispersions of CCTO by angle-resolved photoemission spectroscopy (ARPES) measurements.

II. EXPERIMENTS

ARPES experiments were performed at the beamline BL5U of UVSOR, using photon energies ($h\nu$) from 30 to 93 eV. Measurements were carried out at room temperature ($T = 300$ K) in a vacuum better than 2×10^{-8} Pa. Total energy resolution (ΔE) and momentum resolution (Δk) are about 165 meV and 0.02 $Å^{-1}$ at $h\nu = 90$ eV, respectively. The surface of CCTO prepared by *in situ* cleaving has been very stable during a typical measurement period of 12 h, showing no sign of the progress of degradation. In addition, the detailed electronic structure near E_F has been investigated by the low-energy angle-integrated photoemission spectroscopy (AIPES) measurements at the beamline BL7U, using $h\nu = 7$ eV with $\Delta E \sim 15$ meV.

III. RESULTS AND DISCUSSION

Figure 1(a) shows the energy distribution curves (EDCs) of CCTO in the valence-band region. The spectra have been obtained at room temperature ($T = 300$ K) with changing $h\nu$ from 30 to 93 eV in the normal emission to the (100) plane. With increasing $h\nu$, ARPES spectra trace the blue arrow along the Δ direction in the Brillouin zone of CCTO as depicted in Fig. 1(c). For the sake of convenience, the valence bands are divided into three regions: 0–2.5 eV, 2.5–5 eV, and 5–8 eV. The bands in the regions of 2.5–5 eV and 5–8 eV relatively highly disperse with intense features, while the bands in the region of 0–2.5 eV are not well distinguished due to weak intensity and broad band width. In the region of 0–2.5 eV, we observe the intensity variation of the small shoulder as a function of $h\nu$ (A). The shoulder of A becomes prominent with changing $h\nu$ from 30 to 60 eV, and then its intensity become smaller from $h\nu = 60$–90 eV. This indicates that $h\nu = 60$ eV can be a high symmetry point, even though we should be careful of the variation of the photoionization cross section (σ) with

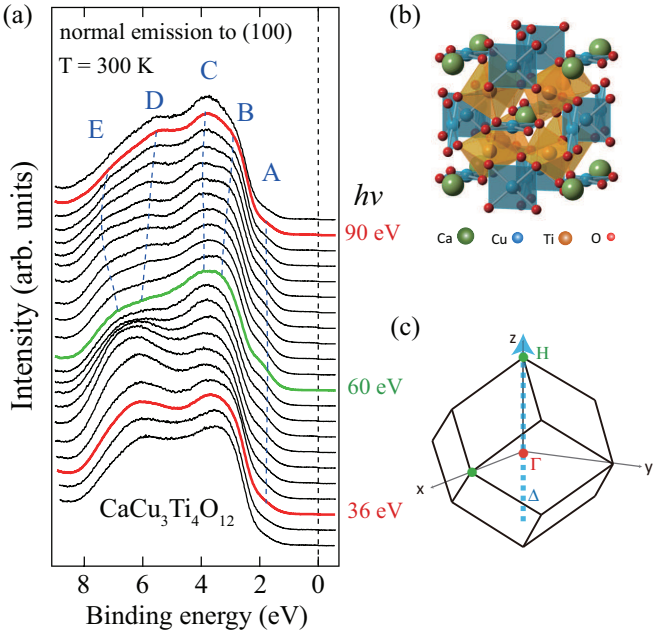

FIG. 1. (Color online) (a) The EDCs along the $\Gamma H(\Delta)$ direction in the normal emission to the (100) plane, observed by using the photon energies from 30 to 93 eV at intervals of 3 eV. The blue dashed lines are guides for the eyes. (b) Body-centered cubic structure (Ref. 10) and (c) Brillouin zone of *A*-site ordered perovskite $CaCu_3Ti_4O_{12}$.

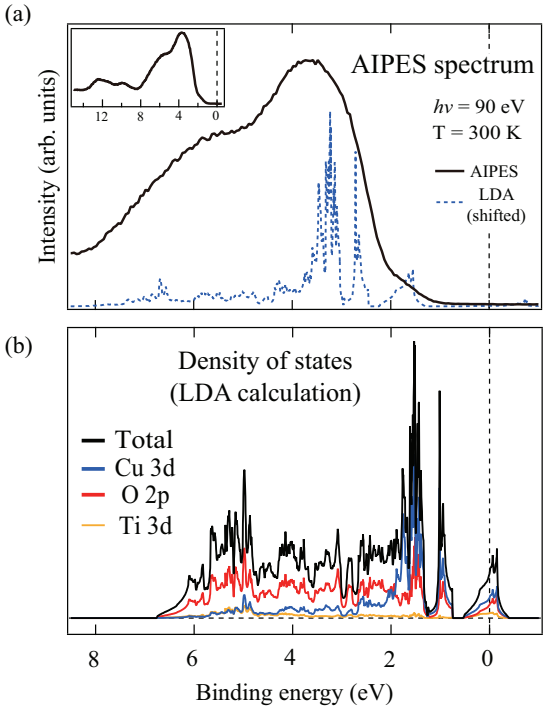

FIG. 2. (Color online) (a) AIPES spectrum of CCTO obtained at $h\nu = 90$ eV and $T = 300$ K in the valence band region. The inset shows the AIPES spectrum in the wide valence band region. For comparison, the partial DOS of Cu 3*d* is inserted below the AIPES spectrum. (b) Total DOS and the partial DOS for the valence bands of Cu 3*d*, O 2*p*, and Ti 3*d* in the LDA calculations.

$h\nu$ caused by Fano resonances, Cooper minima, Auger peaks, etc.[12]

In the region of 2.5–5 eV, there are two types of bands designated by the letters B and C. The band B disperses from 3 to 2.5 eV with the top at $h\nu = 90$ eV and the bottom at $h\nu = 60$ eV, while the band C shows very small dispersion around 3.8 eV reflecting the localized character. In the region of 5–8 eV, bands well split into two types (D and E). As $h\nu$ closes to 90 eV, the band D has the top at 5 eV and the band E has the bottom at 7 eV. From the above results and the analysis based on the free-electron final-state model,[12] we determined the high symmetry points [Fig. 1(a)]: the EDCs at $h\nu = 36$ and 90 eV correspond to the Γ point (red line) and that of $h\nu = 60$ eV to the H point (green line). Beyond the above band dispersion, there is large intensity variation around 6.5 eV as $h\nu$ closes to about 50 eV. Such behavior has also been observed in the other transition-metal oxides, where it comes from the resonance around the O 2*p* edge and is not relevant to band dispersion.[13] At the same time, this means that the spectral weight includes much weight of the O 2*p* orbital in this region.

Let us compare the spectral weight obtained in the angle-integrated mode of analyzer with the density of states (DOS) in the LDA calculations. Figures 2(a) and 2(b) show the AIPES spectrum at $h\nu = 90$ eV and the partial DOS obtained from the LDA calculations, respectively. First, we recognize that the spectral weights near E_F do not seem to exist in this scale plot (actually, there are very small spectral weights, and we will discuss it later) explaining the insulating properties of the electrical resistivity experiments, while the DOS of mainly Cu 3*d* and O 2*p* states exist at E_F in the LDA calculations. When we compare the ARPES spectra with the DOS, the variation of σ with $h\nu$ should be taken into account: the σ of the *d* orbital is generally much larger than that of the *p* orbital by about ten times at $h\nu = 90$ eV.[14] In Fig. 2(a), we plot the partial DOS of Cu 3*d* of the LDA calculations inside the AIPES spectrum, which was shifted to higher binding energy by 1.7 eV. The AIPES spectrum shows good agreement with the shifted partial DOS of Cu 3*d* in the LDA calculations. We find that the shoulder around 2 eV with weak intensity (band A) corresponds to the DOS at E_F in the LDA calculations. There are intense peaks in the region from 2.5 to 8 eV, which correspond to the bands B, C, D, and E in Fig. 1(a). The bands B and C mainly consist of Cu 3*d* states, and the bands D and E mainly come from O 2*p* states. On the other hand, most DOS of the Ti 3*d* orbital are located in the unoccupied region [Fig. 2(b)]. In the inset of Fig. 2(a), we have observed two peaks around 8–13 eV, which do not appear in the LDA calculations. These peaks are the intrinsic features of CCTO, because the peaks have appeared in the fresh surface just after the cleaving sample and show no degradation during the measurements. In fact, it has been reported in CuO, family compound CCRO, etc., that such high-energy peak structures come from Cu $3d^8$ final states due to multiplet effects, indicating atomiclike behaviors caused by strong correlation effects.[7,15–17]

Figure 3(a) shows EDCs obtained in the angle-resolved mode of analyzer at $h\nu = 90$ eV and $T = 300$ K. Geometrically, the direction of the spectra is parallel to the sample surface (namely, perpendicular to the normal emission) and is also along the Δ direction due to the symmetry of the cubic structure. Hence, both EDCs in Fig. 1(a) and in Fig. 3(a)

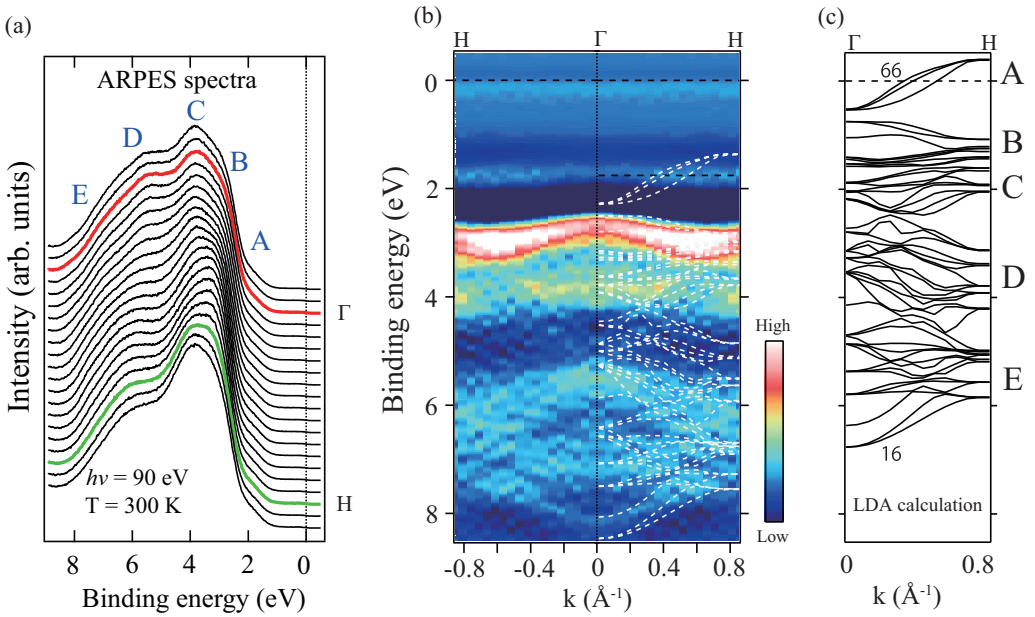

FIG. 3. (Color online) (a) ARPES spectra of CCTO along the Δ direction in the parallel to the cleaved surface (100) plane at $h\nu = 90$ eV and $T = 300$ K. (b) ARPES image obtained from the second derivatives of the EDCs. The theoretical band dispersions (white dashed line), shifted by 1.7 eV, are plotted on the ARPES image. (c) Theoretical band dispersions obtained from the LDA calculations.

represent the same band dispersions. Certainly, we recognize that the EDCs of the $h\nu$-dependent photoemission spectroscopy (PES) from 60 to 90 eV are very similar to the ARPES spectra, indicating the same band dispersions. At the same time, this means that the estimation of the symmetry points is appropriate and our experimental results are reliable. By comparing these two kinds of photoemission spectra with the band calculations, we can explicitly determine the band dispersion of CCTO. Figure 3(b) is the image of the ARPES spectra obtained by the second derivatives of the EDCs. Figure 3(c) shows the band dispersions obtained from the LDA calculations. And, the calculated band dispersions are superimposed on the ARPES image, shifting to the higher binding energy by 1.7 eV [Fig. 3(b)]. First, it should be noted that there are 51 bands in the valence-band region as shown in Fig. 3(c). Unfortunately, the PES experiments cannot resolve these bands very close to each other due to the limitation of ΔE and Δk. Therefore, the observed five types of band dispersions (A, B, C, D, and E) in ARPES experiments should be interpreted as a bundle of bands with similar tendency. In the region of 0–2.5 eV, the EDCs show a little different behavior between ARPES and $h\nu$-dependent PES. The intensity variation of band A around 2 eV in the ARPES measurements [Fig. 3(a)] is small compared to the $h\nu$-dependent PES measurements [Fig. 1(a)], which may come from the different transition probability between the initial state and final state in the different methods of PES measurements. As discussed in Fig. 2(a), we can assign band A to three bands from 64 to 66 which cross E_F and show the band dispersion of about 1 eV [Fig. 3(c)]. Even though the exact size of band dispersion cannot be estimated due to the band broadening in the ARPES measurements, we find that the band width in ARPES is very narrow compared to the LDA calculations [Fig. 3(b)]. This indicates that band A has the larger effective mass and is more localized than the expectation of the LDA calculation, as observed in strongly correlated f-electron systems.[18] According to the Mott-Hubbard model, the large repulsive Coulomb interaction separates the DOS into the upper Hubbard band in the unoccupied region and the lower Hubbard band in the occupied region.[7] In the case of CCTO, the hybridized bands of Cu $3d$ and O $2p$ states were shifted to the higher binding energy by about 1.7 eV in comparison with the LDA calculations, showing a little different behavior compared to the simple Mott-Hubbard model. However, this is not surprising because the Cu $3d$ states have about nine electrons in the occupied region and about one electron in the unoccupied region and are well hybridized with O $2p$ states in spite of the strong correlation effects. In fact, the similar band structures can be found in earlier studies of CuO and the high-T_c cuprates.[7,15] In the region of 2.5–5 eV, band C disperses from 3.8 eV at the Γ point (red line) to 3.5 eV at the H point (green line) showing small upturn behavior [Fig. 3(a)]. Around 2.7 eV, there is a shoulder which corresponds to band B. Bands B and C are assigned to bands from 60 to 63 and bands from 55 to 59, respectively. In the region of 5–8 eV, the ARPES data show the well-split bands, D and E. We find that these bands consist of many bands from 16 to 50, even though it is difficult to observe the bands around 5 eV.

Consequently, the tendency of band dispersions of ARPES experiments is very consistent with those of the LDA calculations, except for the band shifting to the higher binding energy by about 1.7 eV, the band narrowing around 2 eV, and the high-energy multiplet structures of Cu $3d^8$ final states around 8–13 eV. And these different electric structures can be assigned to the strong correlation effects. In addition, it should be noted that the obtained ARPES results are worthy of comparison with other theoretical studies such as LDA + U (U: on-site Coulomb interaction) and dynamical

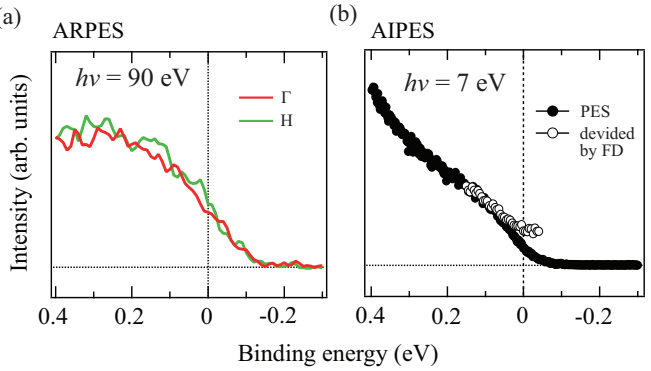

FIG. 4. (Color online) (a) The enlarged ARPES spectra at the Γ and H points near E_F in Fig. 3(a). (b) The bulk sensitive AIPES spectra near E_F at $h\nu = 7$ eV. The solid circle is the AIPES sepctrum and the open circle is the spectral weight near E_F obtained from dividing the AIPES spectrum by the convoluted Fermi-Dirac function ($\Delta E \sim 15$ meV and $T = 300$ K).

mean field theory (DMFT) calculations which include the strong correlation effects.

Finally, let us discuss the small spectral weights at E_F. Figure 4(a) is the enlarged plot of EDCs at the Γ and H points in Fig. 3(a). We find that there is a very small spectral weight at E_F in spite of the insulating phase in the electrical resistivity measurements. Several possibilities can be considered in analysis and interpretation. A possibility, Ti $3d$ states remain at E_F, should be ruled out because CCTO would show the metallic properties if Ti $3d$ states exist at E_F. Another possibility is that the metallic phase is caused by the surface state of CCTO, because the PES spectra, obtained by using $h\nu = 20$–100 eV, are surface sensitive as explained by the universal curve.[19] It is well known that the mean free path (λ) in solids becomes long enough to probe the bulk properties by using the low $h\nu$ ($\lambda \sim 200$ Å at $h\nu = 7$ eV).[19,20] Therefore, we have performed the AIPES measurements at $h\nu = 7$ eV as shown in Fig. 4(b). The spectral weight at E_F (open circle) has been recovered by dividing the AIPES spectra (solid circle) by the Fermi-Dirac function convoluted by the energy resolution and the measurement temperature.[18,21] There exist unambiguous spectral weights at E_F. This indicates the strong possibility of the density of states in bulk. Actually, the hopping conductivity has been observed in the electrical resistivity measurements.[22] For the explanation of both the PES and electrical resistivity measurements, the existence of isolated metallic states in bulk is very reasonable. Of course, it should also be noted that the low-$h\nu$ AIPES results do not mean no surface states at E_F, because we still cannot completely rule out the surface states, even though the spectra at $h\nu = 7$ eV almost reflect the bulk states.

Generally, disorders and/or defects can be considered as possible origins. For example, such metallic states are often observed in cuprates due to oxygen defects. Recently, Zhu *et al.* have showed that disorder causes the metallic states in CCTO by quantitative electron diffraction and extended x-ray absorption fine structure studies.[4] They have reported that Cu and Ca atomic substitution gives rise to nanoscale metallic states, which has been suggested as one of the origins of the extremely large ϵ. As mentioned above, the origin of the intriguing spectral weight at E_F and its relation with the high ϵ are important subjects and should be further studied.

IV. SUMMARY

We have performed ARPES measurements in A-site ordered perovskite CCTO and directly observed the clear band dispersions. In comparision with the LDA calculations, the ARPES results show agreement in the overall electronic structures but different features in the detailed electronic structures, i.e., band shifting of about 1.7 eV to the higher binding energy, band narrowing around 2 eV, and high-energy multiplet structures around 8–13 eV. And, we have assigned these to the strong correlation effects of the Cu $3d$ electrons well hybridized with O $2p$ states. At E_F, very small spectral weights have been observed in the insulator phase, which indicates the existence of isolated metallic states.

ACKNOWLEDGMENT

The authors are grateful to M. Sakai and S. Nakajima for technical assistance.

*hojun@cc.hirosaki-u.ac.jp

[1] M. A. Subramanian, D. Li, N. Duan, B. A. Reisner, and A. W. Sleight, J. Solid State Chem. **151**, 323 (2000).
[2] C. C. Homes, T. Vogt, S. M. Shapiro, S. Wakimoto, and A. P. Ramirez, Science **293**, 673 (2001).
[3] S. Y. Chung, I. D. Kim, and S. J. L. Kang, Nat. Mater. **3**, 774 (2004).
[4] Y. Zhu, J. C. Zheng, L. Wu, A. I. Frenkel, J. Hanson, P. Northrup, and W. Ku, Phys. Rev. Lett. **99**, 037602 (2007).
[5] A. P. Ramirez, M. A. Subramanian, M. Gardel, G. Blumberg, D. Li, T. Vogt, and S. M. Shapiro, Solid State Commun. **115**, 217 (2000).
[6] A. P. Litvinchuk, C. L. Chen, N. Kolev, V. N. Popov, V. G. Hadjiev, M. N. Iliev, R. P. Bontchev, and A. J. Jacobson, Phys. Status Solidi A **195**, 453 (2003).
[7] M. Imada, A. Fujimori, and Y. Tokura, Rev. Mod. Phys. **70**, 1039 (1998).
[8] G. Kotliar, S. Y. Savrasov, K. Haule, V. S. Oudovenko, O. Parcollet, and C. A. Marianetti, Rev. Mod. Phys. **78**, 865 (2006).
[9] L. He, J. B. Neaton, M. H. Cohen, D. Vanderbilt, and C. C. Homes, Phys. Rev. B **65**, 214112 (2002).
[10] Y. W. Long, N. Hayashi, T. Saito, M. Azuma, S. Muranaka, and Y. Shimakawa, Nature (London) **458**, 60 (2009).
[11] W. Kobayashi, I. Terasaki, J. ichi Takeya, I. Tsukada, and Y. Ando, J. Phys. Soc. Jpn. **73**, 2373 (2004).
[12] S. Hüfner, *Photoelectron Spectroscopy* (Springer, Berlin, 2003).
[13] K. Breuer, D. M. Goldberg, K. E. Smith, M. Greenblatt, and W. McCaroll, Solid State Commun. **94**, 601 (1995).

[14]J. J. Yeh and I. Lindau, At. Data Nucl. Data Tables **32**, 1 (1985).
[15]J. Ghijsen, L. H. Tjeng, J. van Elp, H. Eskes, J. Westerink, G. A. Sawatzky, and M. T. Czyzyk, Phys. Rev. B **38**, 11322 (1988).
[16]H. Eskes, L. H. Tjeng, and G. A. Sawatzky, Phys. Rev. B **41**, 288 (1990).
[17]N. Hollmann, Z. Hu, A. Maignan, A. Günther, L.-Y. Jang, A. Tanaka, H.-J. Lin, C. T. Chen, P. Thalmeier, and L. H. Tjeng, Phys. Rev. B **87**, 155122 (2013).
[18]H. J. Im, T. Ito, H. D. Kim, S. Kimura, K. E. Lee, J. B. Hong, Y. S. Kwon, A. Yasui, and H. Yamagami, Phys. Rev. Lett. **100**, 176402 (2008).
[19]M. P. Seah and W. A. Dench, Surf. Interface Anal. **1**, 2 (1979).
[20]T. Kiss, F. Kanetaka, T. Yokoya, T. Shimojima, K. Kanai, S. Shin, Y. Onuki, T. Togashi, C. Zhang, C. T. Chen, and S. Watanabe, Phys. Rev. Lett. **94**, 057001 (2005).
[21]T. Greber, T. J. Kreutz, and J. Osterwalder, Phys. Rev. Lett. **79**, 4465 (1997).
[22]T. Watanabe (private communication).